Position Prediction of Marine Seismic Streamer Cables using Various Kalman Filter Methods

Jan Vidar Grindheim[1]
1) GEOGRAF AS
Kanalsletta 4
NO-4033 Stavanger, Norway
E-mail: jg@geograf.no

2) REALTEK
Norwegian University of Life Sciences (NMBU)
P.O.B. 5003
NO-1432 Ås, Norway

3) Laboratório de Ondas e Correntes (LOC) at UFRJ/COPPE, Federal University of Rio de Janeiro, Rio de Janeiro 22241-160, Brazil

Inge Revhaug[2]
REALTEK
Norwegian University of Life Sciences (NMBU)
P.O.B. 5003
NO-1432 Ås, Norway
E-mail: inge.revhaug@nmbu.no

Egil Pedersen[3]
Department of Engineering Science and Safety
UiT - The Arctic University of Norway
Hansine Hansens veg 18
NO- 9037 Tromsø, Norway
E-mail: egil.pedersen@ntc-as.no

Peder Solheim[4]
Geograf AS
Kanalsletta 4
NO-4033 Stavanger, Norway
E-mail: peder@geograf.no

ABSTRACT

Towed seismic streamer cables are extensively employed for offshore marine petroleum exploration. With the increasing need for accurate streamer steering due to rising number and length of streamers and decreasing intra-streamer separation, as well as new types of survey configurations, accurate modeling, positioning and path prediction of the streamers is imperative. In the present study, a

[1] Corresponding author; Industrial PhD student.
[2] Professor of Mathematics and Head Supervisor of corresponding author.
[3] Professor of Technology and Co-supervisor of corresponding author.
[4] Industrial PhD mentor of corresponding author and CEO of Geograf AS.

variety of models and methods have been implemented and utilized for data assimilation of full-scale seismic streamer position data for a marine seismic streamer, followed by path prediction ahead of time. The methods implemented are described, including various models used with the Kalman filter, Extended Kalman filter and Ensemble Kalman filter, with comparison and evaluation of prediction results. One particular method, the Path-In-the-Water Ensemble Kalman filter (PIW-EnKF), appears to be the most robust method with good prediction results compared to the other methods, as well as having low computational cost. As a case study with full-scale data, the PIW-EnKF is further employed for estimation and prediction of a complete streamer spread.

Keywords

Seismic streamer modeling, Seismic navigation, Data assimilation, Model prediction, Parameter estimation.

INTRODUCTION

In marine seismic surveys, a number of streamers of up to 12 km length are towed behind a vessel (Fig. 1). At specific time intervals (shotpoints), typically equivalent to about 20 m sailing distance, pneumatic sources located between streamer spread and vessel fire, generating sound waves that are reflected by the earth strata and recorded by numerous pressure-sensitive sensors spaced along the streamers. Based on the collected data, images of the local strata structures can be generated in order to indentify traps for hydrocarbon resources.

During the survey, cable node positions are determined based on Kalman filtering measurements from instruments like acoustic devices, gyrocompasses and satellite positioning systems. Wing devices called birds are spaced typically ~300 m apart along the streamers in order to provide lateral and depth control. The main reasons for lateral steering, which by now has became industry standard, is to

- control the desired intra-streamer separation and shape of the streamer spread,
- avoid entangling of cables, especially as the industry trend is larger number of cables with narrower intra-streamer separation, and

- improve 4D-surveys by being able to follow the historic streamer positions more closely.

The present study intends to improve position prediction capability for streamers, which is important for efficient lateral streamer steering [1,2].

In Grindheim et al. [3], a 3D cable dynamics model, solved with a finite difference method (FDM), was utilized with the Ensemble Kalman Filter (EnKF) and Ensemble Kalman Smoother (EnKS) for data assimilation and prediction by application of synthetic data. In Grindheim et al. [4], the 3D model was reduced to 2D by assuming constant cable depth. Furthermore, a 2D Path-In-the-Water (PIW) model was developed, and the two 2D models were utilized with the EnKF for data assimilation and prediction using full-scale seismic streamer data.

In the present study, a comparison is performed between various models and Kalman filter variants implemented in MATLAB [5] for the estimation and prediction of a seismic streamer path. The data utilized are based on processed full-scale seismic streamer position data (P1-data) for one streamer. Estimation is performed on the first 8 minutes followed by a 6 minutes prediction. The predicted position results are presented, comparing the performance of the implemented filters. Finally, for the method giving the overall best result, estimation followed by a 15 minute prediction of the complete streamer spread is demonstrated. Results are compared to the full-scale streamer spread data.

FULL-SCALE DATA

The full-scale data used in this study are the same as in Grindheim et al. [4]; processed position data (P1-data) from a seismic survey. Streamer position data at the very start of the survey line are utilized. Shotpoint interval is 8 seconds. Streamer nominal length is 5987.5 m, with 49 data nodes spaced 125 m nominal streamer length apart except to the last node, where spacing is 112.5 m [4]. Presently the data used is increased from 10 minutes (75 shotpoints) to 14 minutes (105 shotpoints) for the comparison study [4]. The first 8 minutes are used for data assimilation, followed by 6 minutes prediction, where predicted and data positions are compared for the different methods. In the comparison study, one of the streamers is employed.

For the final case study, estimation and prediction for all 8 streamers is shown for the method giving the best results. In this case study, 23 minutes (173 shotpoints) data are employed, i.e. 8 minutes estimation and 15 minutes prediction. Simulated position measurements are generated by adding white measurement noise to the P1-coordinates. The processed P1-coordinates have been verified against observations using the seismic navigation Quality Control software ResProg [6].

METHODOLOGY

The filter variants utilized in this study are the Kalman filter (KF), Extended Kalman filter (EKF) and Ensemble Kalman filter (EnKF). Various models are implemented, and each model is employed in one or two of the filter types. Subsequently, each resulting filter has been employed on the data for data assimilation and estimation until shotpoint 59 followed by prediction until shotpoint 105. In the following section, the prediction results will be compared for the various filters. Position measurement noise is set to 1 m and the front node is considered known.

PIW-EnKF

The PIW-EnKF (Path-In-the-Water – Ensemble Kalman filter) was presented in Grindheim et al. [4]. The Path-In-the-Water (PIW) model is based on the assumption that node #2, i.e. the node downstream of the front node, will follow the front node's path, node #3 will follow node #2's path, and so forth [4]. In addition, an offset angle α has been included, correcting for path deviations resulting from factors like ocean current and bird steering. α is estimated as a parameter in the EnKF, updated at data assimilation steps [7].

The EnKF "is a sequential Monte Carlo method that provides an alternative to the traditional Kalman filter (KF)" [7]. Instead of propagating the state error covariance matrix forward in time, an ensemble of model realizations are integrated individually forward in time. This also leads to the avoidance of linearization for nonlinear model dynamics, which is required with the Extended KF (EKF) [8].

For estimation of α, white noise of standard deviation 0.1 radians with decorrelation distance γ along cable of $10^4/3$ m is used [4]. Position process noise has standard deviation 1.5 m.

One major approximation in the EnKF is the finite number of model realizations in the ensemble [7]. Obviously, there is a trade-off between ensemble size and processing time. Monte Carlo methods such as the EnKF converge with $\sqrt{n_e}$, thus convergence is slow [7]. To investigate the effect of number of model realizations in the ensemble (n_e), the PIW-EnKF with different values of n_e, keeping all other settings constant, was applied with the present data. The parameter estimation results of α for increasing values of n_e are presented in Fig. 2, showing estimated α at first prediction step (shotpoint 60). This α is used for all prediction steps.

In Table 1, sum of absolute difference to estimated $\alpha_{n_e=20,000}$ is given for the different options plotted in Fig. 2. It shows that n_e has an impact on the estimated α; however, the results indicate that the improvement is relatively small for $n_e >$ ~500 (Fig. 2, Table 1). In the prediction results presented in Figs. 3~4, n_e=500 has been utilized for all EnKFs.

For the prediction, i.e. shotpoint 60 through 105, the complete ensemble has been integrated forward in time. This gives an "optimal" prediction estimate with uncertainty estimate [9]. However, a quick forecast solution has also been implemented, which integrates only one single model realization forward in time, starting from the ensemble mean or alternatively the ensemble median [9]. This routine is computationally fast, but it does not accommodate uncertainty estimate since only one model realization is integrated. It should also be less accurate compared to integrating the complete ensemble forward in time.

Prior to prediction, which starts at shotpoint 60, the RTS smoother algorithm is utilized for smoothing the estimated α, i.e. the mean of the α-ensemble [4,8].

The *improvedist* feature, which adjusts the straight-line distances between streamer nodes to correspond to the nominal node spacing, is utilized for prediction steps [4]. The *improvedist* feature has been shown to improve the result for the PIW-EnKF when used for prediction steps only [4].

PIW-EKF

An Extended Kalman filter (EKF) with the same PIW-model as employed in the PIW-EnKF has also been implemented. White noise is used in the estimation of α, but with a decorrelation distance γ along the cable so that the noise for all estimated values of α are correlated [4]. As for the PIW-EnKF, process noise for α is set to standard deviation 0.1 radians, but with decorrelation distance increased to γ=30,000 m. These values are also used for initial covariance. It was found that a large value of γ giving a high correlation in distance is needed for the estimated values of α to be fairly smooth. Even with the currently high setting of γ in the PIW-EKF, a see-saw-pattern in the estimated α can still be noticed (Fig. 2). In the PIW-EnKF, a significantly lower decorrelation distance of $\gamma=10^4/3$ m is used, which may be more appropriate if large cable deflections, as well as significant spatial deviations in ocean currents and other disturbances, are to be accounted for, which is necessary for a robust system [4]. Especially for the full scale data in question, this lower setting of γ is assumed to be more realistic, as ocean currents appear to vary significantly along the streamers.

Model position error has standard deviation 1.5 meters per step, as for the PIW-EnKF. Transition matrix Φ is used for forward integration of both α and state covariance matrix, while forward integration of node positions is performed directly with the PIW-method to avoid the linearization approximation.

As for the PIW-EnKF, the *improvedist* feature is utilized for prediction steps [4]. However, the *improvedist* feature is not included in the model linearization as this would complicate matters considerably. This leads to a discrepancy in forward integration of both state covariance and parameter α. This discrepancy is avoided with the PIW-EnKF, since the EnKF avoids linearization and propagation of an error covariance matrix [7].

p-v-a Kalman filter

A position-velocity-acceleration Kalman filter (p-v-a-KF) has been implemented. In the p-v-a-KF, the derivative of acceleration is a 1st order Gauss-Markov signal with standard deviation σ and decorrelation time τ [8]. p is local node position, the front node being the origin. v is node velocity and a is node acceleration.

The basic *p-v-a* model is utilized individually for each coordinate on each of the 49 cable nodes, thus assuming no correction between nodes. However, various options for adding correlations between the nodes were examined, using different noise settings as well as different methods. Best results were obtained by using the *RTS-cable* option on all steps, and *improvedist* as well for prediction steps. *RTS-cable* filters cable node coordinates using the RTS smoother algorithm applied along the cable [8]. Both inline and crossline coordinates are RTS filtered, using a 2-state 1st order Gauss-Markov filter with distance correlation, smoothing the cable's shape. Attempts were also made to implement distance correlations directly in the process noise **G**-matrix [8]; however, result improvements were not achieved.

FEM-EnKF based on Türkyilmaz [10, p. 72]

Türkyilmaz [10] employed a Finite Element Method (FEM) to discretize the coupled partial differential equations of 3D-motion (for "small" cable deflections) for a towed underwater cable into a set of ordinary differential equations [10]. This resulted in three equations; for inline, crossline and depth dimensions. These equations could be further simplified by lumping both mass and drag forces of the two neighboring elements at each node. Furthermore, when considering only the crossline (horizontal lateral) direction, the following equations are obtained [10, p. 72]:

$$\begin{aligned} \ddot{y}_n &= \frac{T_n}{m_1 h^2}\left(y_{n-1} - 2y_n + y_{n+1}\right) - \tfrac{1}{2}\rho d C_b m_1^{-1}\left|\dot{y}_n\right|\dot{y}_n \\ \ddot{y}_{end} &= \frac{T_{end}}{m_1 h^2}\left(y_{end-1} - y_{end}\right) - \tfrac{1}{2}\rho d C_b m_1^{-1}\left|\dot{y}_{end}\right|\dot{y}_{end} \end{aligned} \qquad (1)$$

Equation (1) is utilized for calculating acceleration $\ddot{y}$ for node 2 through node *end*. Node 1 is the front node, which is considered known, node 2 is the next node along the cable, and node *end* is the tail node (presently node 49). y is crossline position, whereas $\dot{y}$ is crossline velocity. T is cable tension at the node. Türkyilmaz [10] used instead a fixed tension for the entire cable. Presently, nominal tension calculated using the 3D FDM method described in Grindheim et al. [3] is utilized, based on initial front node velocity. This should improve accuracy compared to employing a fixed cable tension. Virtual mass m_1, i.e. mass plus added mass, where added mass is assumed equal to mass of displaced

water volume, is used since this is for transverse direction [11-13]. ρ is density of water and d is diameter of the cable. C_b is drag coefficient in crossline direction and h is distance between nodes. For the present filter the coordinate system is rotated so that inline direction is close to the front node velocity direction, since this is important for Eqn. (1) to function well. However, for calculating the results (Figs. 3~4), the coordinates are rotated back to the same coordinate system utilized for the other filters.

Euler integration is utilized for the time integration, with timesteps of 0.05 seconds. The integration has been vectorized for integrating all states in the ensemble instantaneously, for computational speed optimization.

Eqn. (1) applies for crossline direction only. In inline direction, the *improvedist* method is employed for all steps, keeping nominal straight-line distance between nodes [4].

FEM-EKF based on Türkyilmaz [10, p. 72]

Further, an Extended Kalman filter (EKF) was implemented based on the crossline model by Türkyilmaz [10], Eqn. (1). The implementation is similar to the corresponding EnKF based on the same model. As in the EnKF, Eqn. (1) is used for the crossline state time integration, using Euler integration with timesteps of 0.05 seconds. For the crossline covariance integration, the Jacobian (the **F**-matrix) is calculated for Eqn. (1), updated each 0.05 seconds, using vanLoan's method to calculate transition matrix Φ and process noise covariance matrix **Q** [8]**.**

In inline direction, the *improvedist* feature is utilized at all steps, additionally adding white noise on acceleration [8]. For the corresponding covariance prediction the white noise is used, while the *improvedist* feature is not included in the linearized covariance prediction. This obviously introduces an anomaly in the EKF, but including the *improvedist* feature in the covariance prediction would complicate matters considerably. Recall that the same approximation was introduced in the PIW-EKF.

Note that a drawback of FEM compared to FDM is that FEM typically is not stable for large timesteps, thus necessitating small timesteps resulting in slower time integration, whereas FDM may

be stable for large timesteps [14,15]. However, FDM models are typically difficult to implement in EKF.

PREDICTION RESULTS

Prediction results at 6 minutes prediction time, i.e. at shotpoint 105, for the various methods described are presented in Fig. 3 for Crossline coordinates, and Fig. 4 for Inline coordinates. For each figure, *M* (maximum coordinate deviation) and *S* (sum of coordinate deviation) according to Eqn. (2) are presented for each prediction result, and the results are sorted according to *M* [4].

$$\begin{aligned} deviation_{coord} &= predicted_{coord} - true_{coord} \\ M &= \max(|\, deviation_{coord} \,|) \\ S &= \sum_{node\#=1}^{49} |\, deviation_{coord}(node\#) \,| \end{aligned} \qquad (2)$$

Comparison of results

p-v-a-KF

The p-v-a-KF was found to be fairly sensitive to noise settings, and results are generally inferior to the other filters except the PIW-EKF (Figs. 3~4). Employing *RTS-cable* improved the results for the present data. This was expected since there in the physical system clearly is a correlation between cable nodes. As for the PIW-EnKF, *improvedist* applied only at prediction steps gave improvement [4].

FEM-EnKF and -EKF

Both the FEM-EnKF and the FEM-EKF give quite good results in comparison to the other filters employed, with only PIW-EnKF being superior (Figs. 3~4). Prediction results for the FEM-EnKF are slightly better than for the FEM-EKF, showing similar results as the PIW-EnKF in crossline direction (Fig. 3). The FEM-EKF is some inferior to the FEM-EnKF, which seems reasonable as approximations are introduced in the covariance propagation in the FEM-EKF with linearization that also excludes the *improvedist* feature incorporated in the model.

PIW-EnKF and -EKF

The PIW-EnKF gives the best results on the present study both for inline and crossline (Figs. 3~4). Especially in inline direction, the results are clearly superior. However, the PIW-EKF gives the least accurate prediction results in the study. The main reason for this appears to be inferiority in parameter estimation of α compared to the PIW-EnKF (Fig. 2). This may be due to the nonlinearities involved in the parameter estimation, since the EKF linearizes around the estimated trajectory. According to Evensen et al. [16], "even for linear dynamics the parameter estimation problem becomes nonlinear and may be extremely difficult to solve." Further, as for the FEM-EKF, the *improvedist* feature is not included in the linearization in the PIW-EKF. Additionally, for the PIW-EKF the distance correlation γ used in the estimation of α was set to an unreasonable high value to achieve a smooth estimate.

Full-scale streamer spread estimation and prediction employing the PIW-EnKF

The PIW-EnKF, which gave the best results for the present study, has been implemented as a MATLAB [5] object capable of estimating and predicting a complete streamer spread consisting of multiple streamers. Included are functionalities for measurement update and for prediction. For measurement update, necessary inputs are observed vessel and streamer node positions with corresponding variances. For prediction, only vessel position, with corresponding variance, for prediction steps are inputs. Offset angle α could be used or not on user's discretion. Object plotting functions have been implemented as well.

To reduce computational time, the prediction ensemble size is by default set to 50 which is significantly smaller than the update ensemble size of n_e=500. Prediction ensemble is generated based on ensemble mean and variance. Ensemble size in prediction is less critical compared to the update step.

The same estimation as previously in this study is run, but in this case, all eight streamers are included. Note that the tail node on streamer #2 has been removed to demonstrate usage with differing number of nodes between individual streamers. Subsequently, prediction for 15 minutes ahead of time is performed for the complete streamer spread, compared to 8 minutes for the previous prediction cases.

Plot of streamer spreads with estimated and predicted positions as well as vessel positions are presented in Figs. 5 and 7. In Fig. 5, α is used in the prediction, whereas in Fig. 7, α is not used. It can be clearly seen that without employing estimated α for prediction, the after sections of predicted streamers almost overlap the estimated streamers, since prediction follows the basic PIW model (Fig. 7), while this is not the case when estimated α is used in the prediction (Fig. 5). In Fig. 5, the predicted streamers instead follow the true streamer positions quite well, although increasing deviations are seen for the aft spread section. Thus, consistent with Grindheim et al. [4], lower offsets between true and predicted streamer positions are shown when estimated α is utilized in the prediction (Fig. 6, lower plots) compared to when α is not utilized (Fig. 8, lower plots).

Estimation results at shotpoint 59 are essentially the same independent of estimating α or not, which is as expected since parameter estimation should not affect coordinate estimation significantly (Figs. 6, 8, upper plots).

On computer runtime, estimation of the present complete streamer spread takes about 0.21 s per step and prediction 0.09 s per step on an average-end laptop.

CONCLUSION

Of the methods employed and investigated, the Path-In-the-Water (PIW) -Ensemble Kalman Filter (EnKF) gave the best results for the present data. The PIW-Extended Kalman Filter (EKF) is not able to estimate offset angle α as accurately as the PIW-EnKF, leading to a significant reduction in prediction accuracy. The Finite Element Method (FEM) -EnKF achieved results that are close to the PIW-EnKF in crossline; however, the PIW-EnKF is computationally faster than both the FEM-EnKF and FEM-EKF. The PIW-EnKF also achieved superior results in inline direction for the present data. For the PIW-EnKF, results consistent with previous findings were achieved when performing estimation followed by prediction 15 minutes ahead of time for the complete streamer spread, which has 8 streamers.

ACKNOWLEDGMENT

Geir Evensen is gratefully acknowledged for support on EnKF, while employed at Statoil (currently Equinor), Bergen, Norway.

This work made part of an Industrial PhD (completed December 2018) at NMBU (Ås, Norway) for Geograf AS (Stavanger, Norway), by the corresponding author. It was funded by Geograf AS and the Research Council of Norway through the Industrial-PhD-program, project #234875. Corresponding author was on leave to Laboratório de Ondas e Correntes (LOC) at UFRJ/COPPE, Rio de Janeiro, Brazil.

REFERENCES

[1] Polydorides, N., Storteig, E., and Lionheart, W., 2008. "Forward and inverse problems in towed cable hydrodynamics," Ocean Engineering, **35**(14), pp. 1429-1438. DOI: 10.1016/j.oceaneng.2008.07.001

[2] Solheim, P., 2013. "Method for determining correction under steering of a point on a towed object towards a goal position," U.S. Patent 8,606,440, issued December 10, 2013.

[3] Grindheim, J.V., Revhaug, I., Pedersen, E., 2017. "Utilizing the EnKF (Ensemble Kalman Filter) and EnKS (Ensemble Kalman Smoother) for Combined State and Parameter Estimation of a 3D Towed Underwater Cable Model," Journal of Offshore Mechanics and Arctic Engineering, **139**, pp. 061303-1~8.

[4] Grindheim, J. V., Revhaug, I., and Pedersen, E., Solheim, P., 2018. "Comparison of Two Models for Prediction of Seismic Streamer State using the Ensemble Kalman filter," Journal of Offshore Mechanics and Arctic Engineering, **140**, pp. 061101-1~9. DOI: 10.1115/1.4040244

[5] MATLAB, *The language of technical computing*, Natick, MA: The MathWorks, Inc.

[6] Vaaland, T., and Solheim, P., 2012. *ResProg 4.5*, GEOGRAF AS, Sandnes, Norway.

[7] Evensen, G., 2009. "The ensemble Kalman filter for combined state and parameter estimation," IEEE Control Systems Magazine, **29**(3), pp. 83-104. DOI: 10.1109/MCS.2009.932223

[8] Brown, R. G., and Hwang, P. Y. C., 1997. *Introduction to Random Signals and Applied Kalman Filtering*, John Wiley & Sons, New York, NY, Chap. 5. ISBN: 978-0-471-12839-7.

[9] Evensen, G., 2009. *Data Assimilation. The Ensemble Kalman filter*, Springer, Berlin, Germany, Chap. 9. ISBN: 978-3-642-03710-8.

[10] Türkyilmaz, Y., 2004. *Modeling and Control of Towed Seismic Cables,* PhD. Norwegian University of Science and Technology, Department of Engineering Cybernetics, ISBN 8247162490.

[11] White, F.M., 2011. *Fluid Mechanics*, 7th ed. McGraw-Hill.

[12] Ablow, C. M., and Schechter, S., 1983. "Numerical Simulation of Undersea Cable Dynamics," Ocean Engineering, **10**(6), pp. 443-457. DOI: 10.1016/0029-8018(83)90046-X

[13] Milinazzo, F., Wilkie, M., and Latchman, S. A., 1987. "An efficient Algorithm for simulating the Dynamics of Towed Cable Systems," Ocean Engineering, **14**(6), pp. 513-526. DOI: 10.1016/0029-8018(87)90004-7

[14] Ersdal, S. 2004. *An Experimental Study of Hydrodynamic Forces on Cylinders and Cables in Near Axial Flow*. PhD, Norwegian University of Science and Technology, Trondheim, Norway.

[15] Burgess, J. J., 1991. "Modeling of Undersea Cable Installation with a Finite Difference Method," Proc. First International Offshore and Polar Engineering Conference, Edinburgh, UK, pp. 222-227.

[16] Evensen, G., Dee, D. and Schróter, J., 1998. "Parameter Estimation in Dynamical Models." In: Chassignet EP, Verron J. (eds.) Ocean modeling and parameterizations. Kluwer Academic, The Netherlands, pp. 373–398.

Figure Captions List

Fig. 1 Example of seismic streamer towing configuration with 20 streamers (a courtesy of Petroleum Geo-Services)

Fig. 2 Upper plot: Estimated α using different number of members in the ensemble (n_e), for the PIW-EnKF, and estimated α for the PIW-EKF, at shotpoint 60. Lower plot: Absolute difference in estimated α compared to $\alpha_{n_e=20,000}$. Lower plot: Absolute difference in estimated α compared to $\alpha_{n_e=20,000}$.

Fig. 3 Crossline coordinate prediction results for the various filters. The legend is sorted according to M (Eqn. (2)).

Fig. 4 Inline coordinate prediction results for the various filters. The legend is sorted according to M (Eqn. (2)).

Fig. 5 Estimated (shotpoint 59) and predicted (shotpoint 173) cable node positions. Estimated α is used in the prediction.

Fig. 6 With α estimated: Estimated standard deviations vs. true deviations for x- and y-coordinates for last measurement updated state (upper plots) and predicted state (lower plots).

Fig. 7 Estimated (shotpoint 59) and predicted (shotpoint 173) cable node positions as in Fig. 5, but now α is not used in the prediction.

Fig. 8 Without α estimated: Estimated standard deviations vs. true deviations for x- and y-coordinates for last measurement updated state (upper plots) and predicted state (lower plots).

Table Captions List

Table 1 Sum of absolute differences between estimated α and estimated $\alpha_{n_e=20,000}$ (PIW-EnKF), for the PIW-EnKF with different n_e-settings, as well as the PIW-EKF, at shotpoint 60 for the dataset.

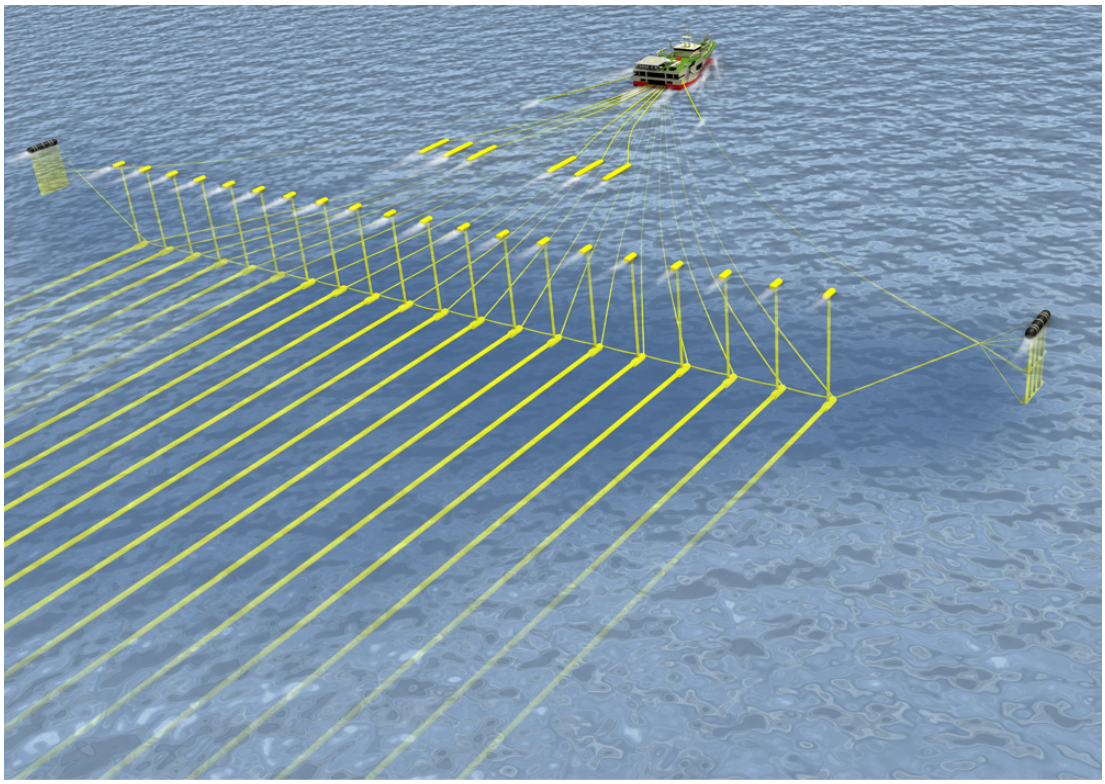

Fig. 1. Example of seismic streamer towing configuration with 20 streamers (a courtesy of Petroleum Geo-Services)

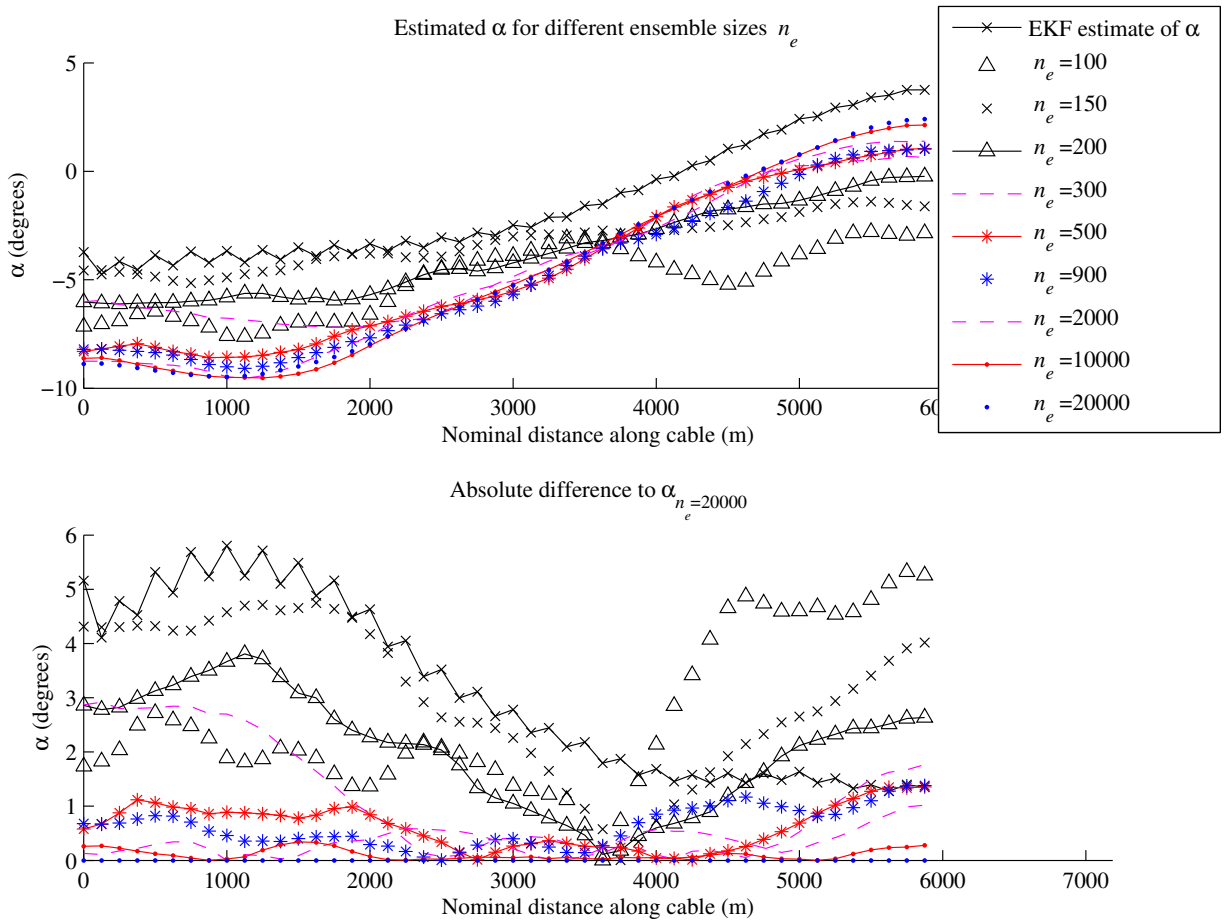

Fig. 2. Upper plot: Estimated α using different number of members in the ensemble (n_e), for the PIW-EnKF, and estimated α for the PIW-EKF, at shotpoint 60. Lower plot: Absolute difference in estimated α compared to $\alpha_{n_e=20,000}$. Lower plot: Absolute difference in estimated α compared to $\alpha_{n_e=20,000}$.

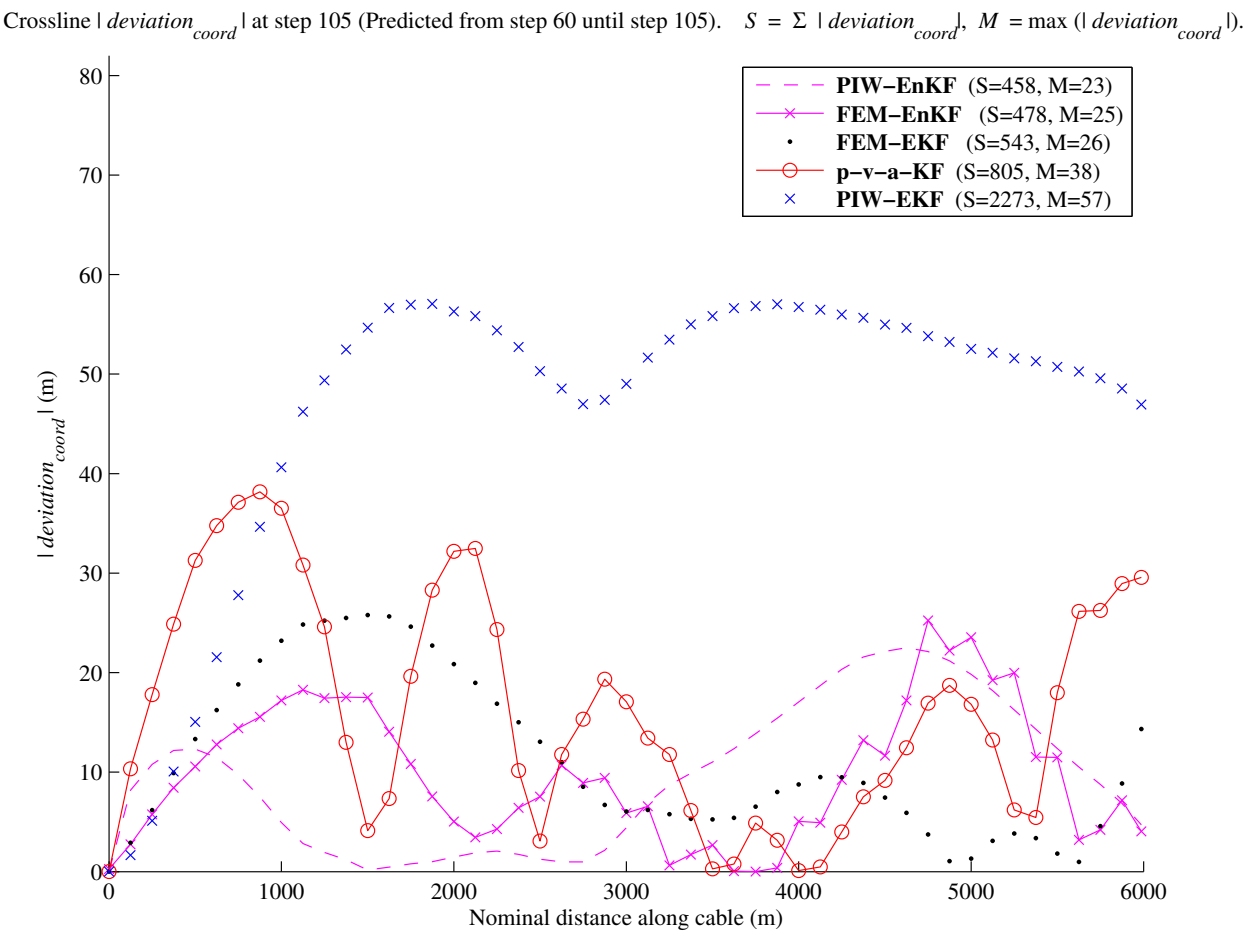

Fig. 3. Crossline coordinate prediction results for the various filters. The legend is sorted according to *M* (Eqn. (2)).

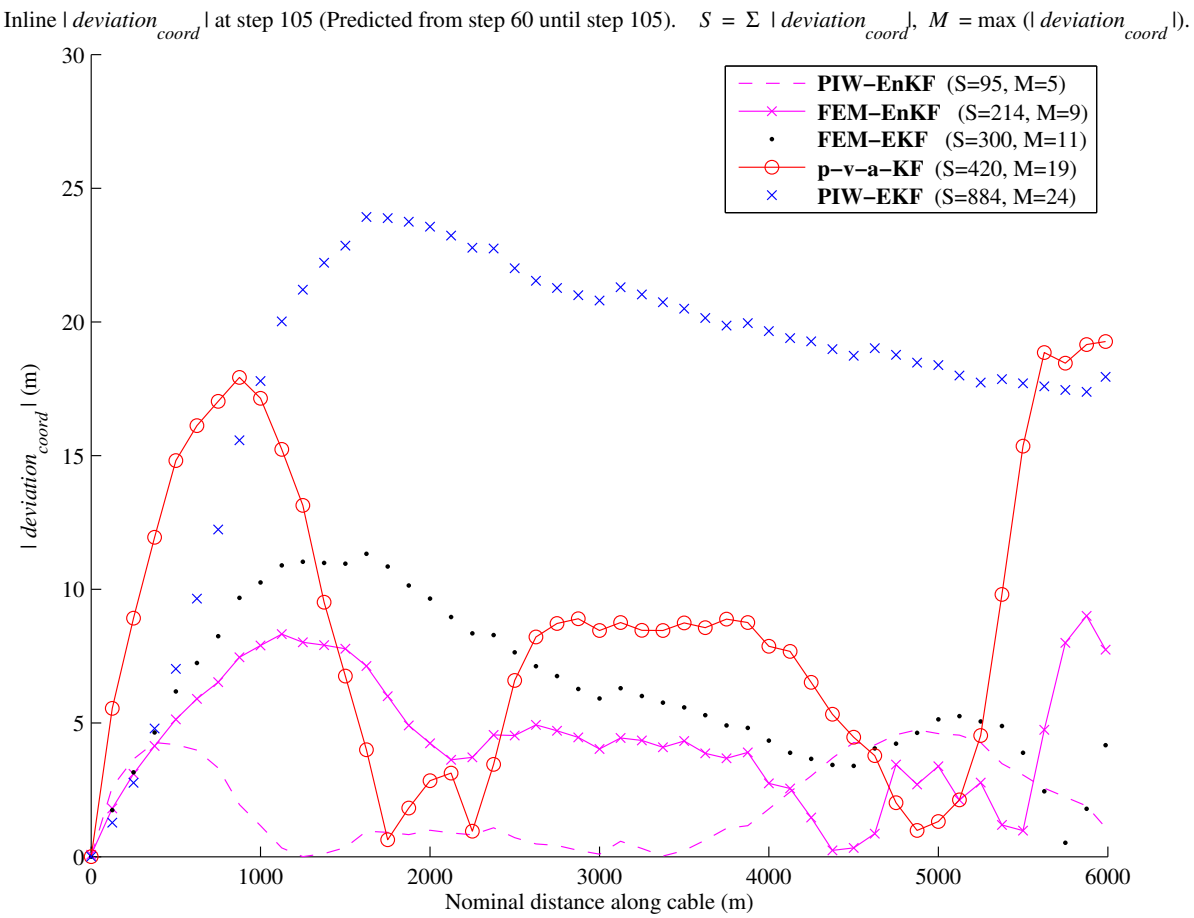

Fig. 4. Inline coordinate prediction results for the various filters. The legend is sorted according to *M* (Eqn. (2)).

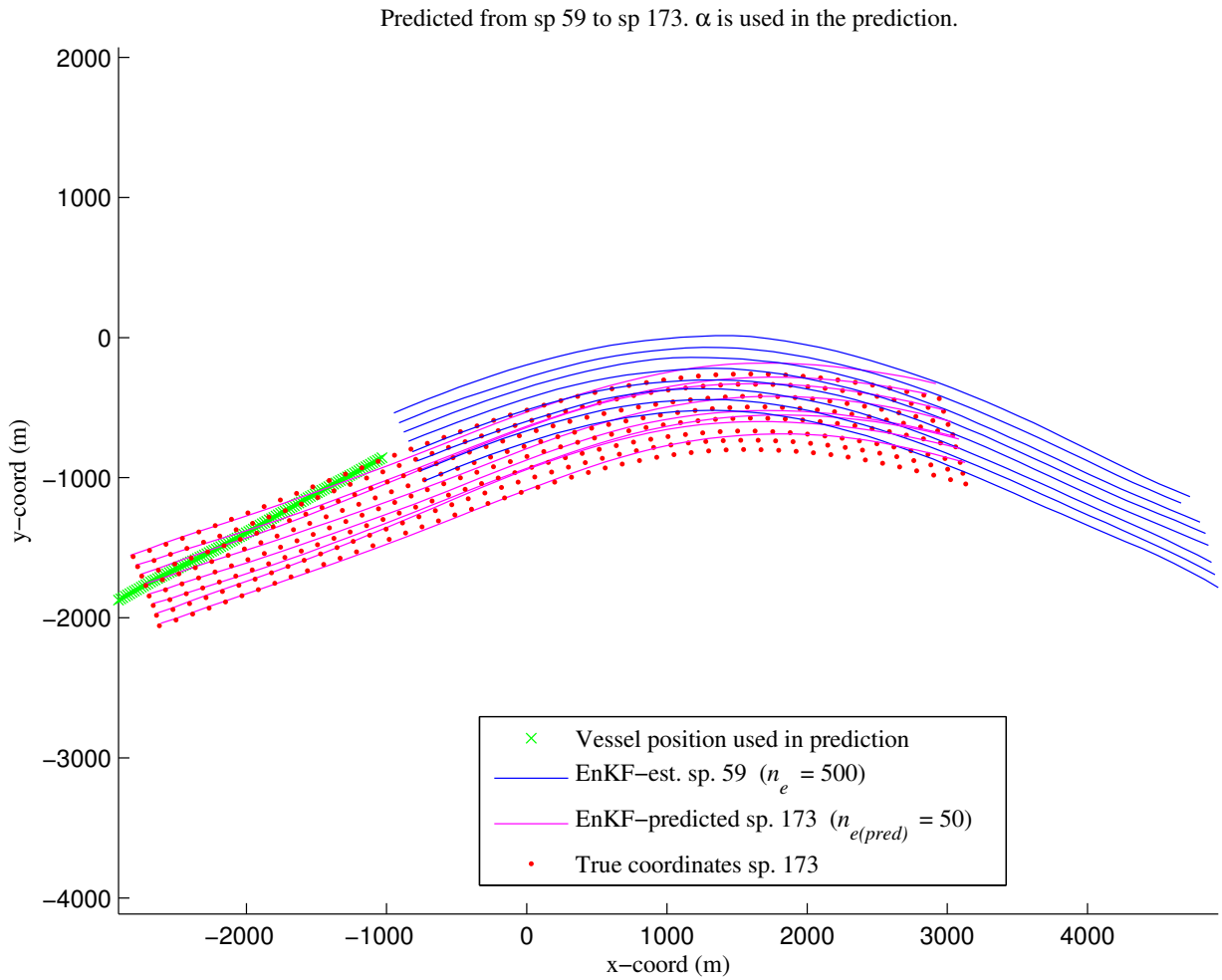

Fig. 5: Estimated (shotpoint 59) and predicted (shotpoint 173) cable node positions. Estimated α is used in the prediction.

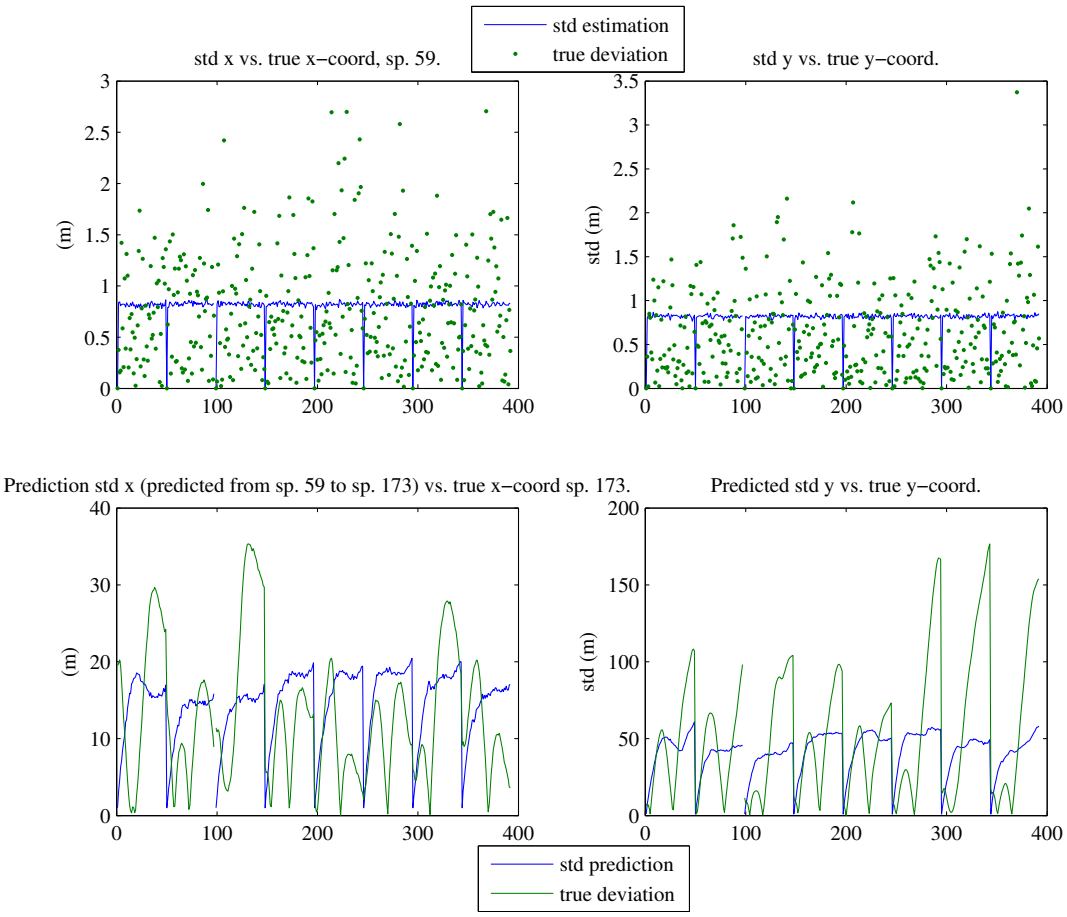

Fig. 6: With α estimated: Estimated standard deviations vs. true deviations for x- and y-coordinates for last measurement updated state (upper plots) and predicted state (lower plots).

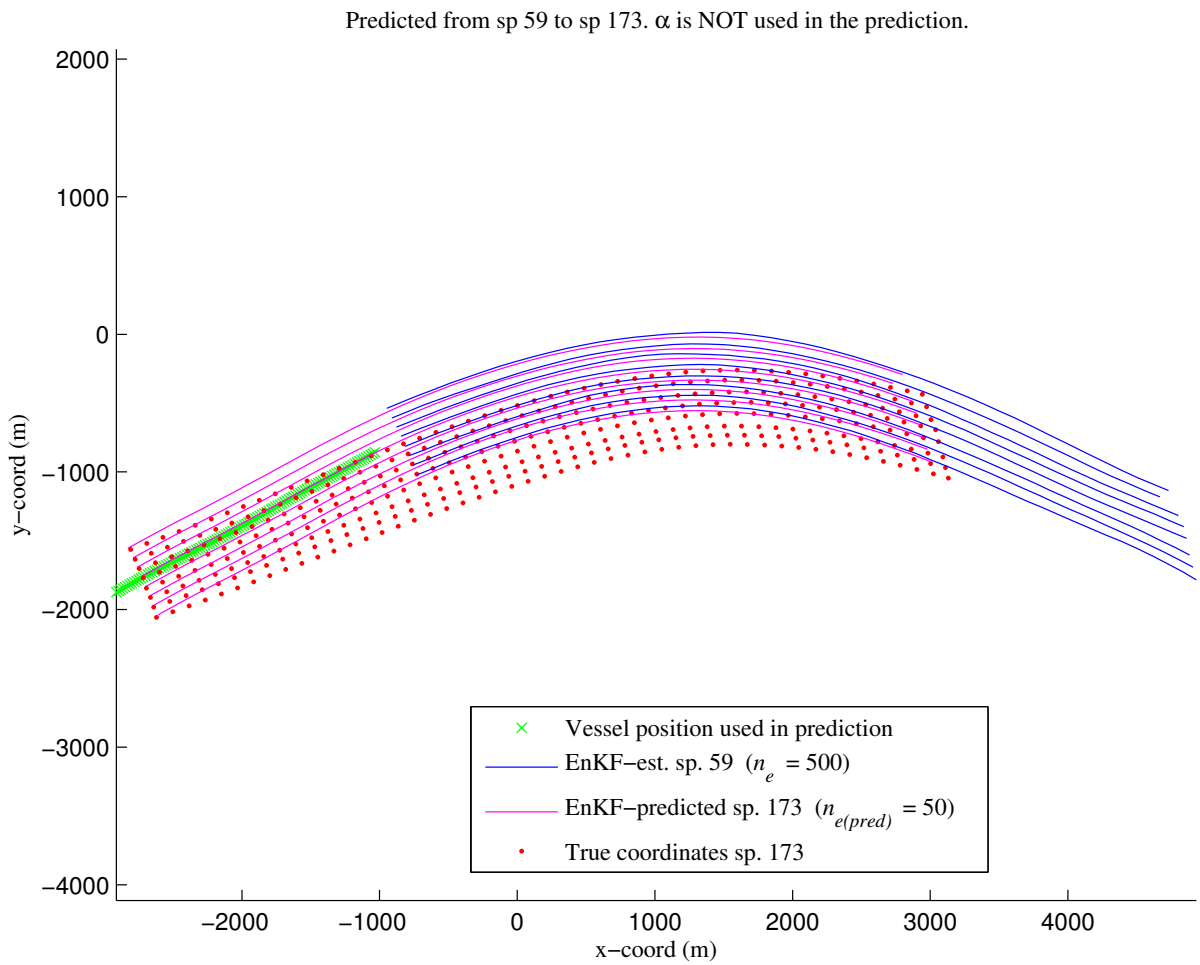

Fig. 7: Estimated (shotpoint 59) and predicted (shotpoint 173) cable node positions as in Fig. 5, but now α is not used in the prediction.

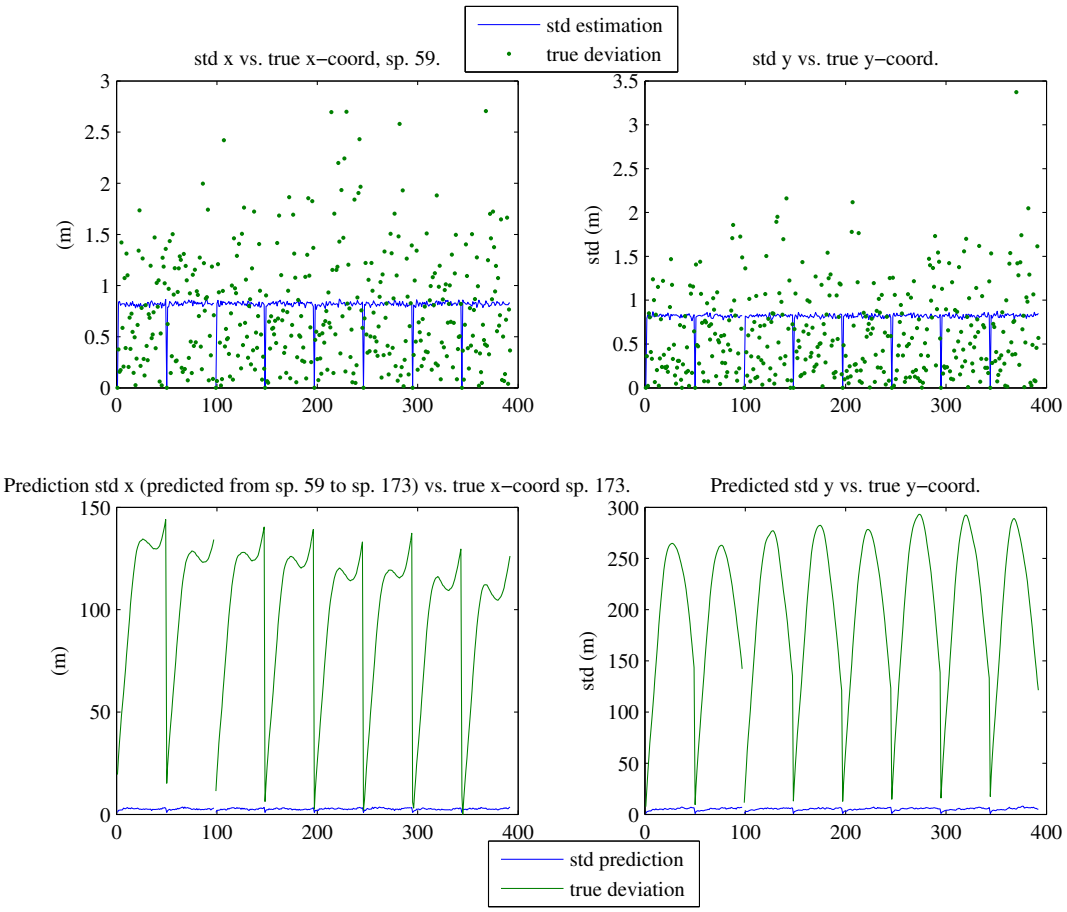

Fig. 8: Without α estimated: Estimated standard deviations vs. true deviations for x- and y-coordinates for last measurement updated state (upper plots) and predicted state (lower plots).

Table 1. Sum of absolute differences between estimated α and estimated $\alpha_{n_e=20,000}$ (PIW-EnKF), for the PIW-EnKF with different n_e-settings, as well as the PIW-EKF, at shotpoint 60 for the dataset.

Description	$\sum\lvert\alpha - \alpha_{n_e=20,000}\rvert$
EKF estimate of α	150.7
n_e=100	125.3
n_e =150	145.1
n_e=200	98.4
n_e=300	55
n_e=500	30.1
n_e=900	29.9
n_e=2,000	16.8
n_e=10,000	5.2
n_e=20,000	0